crystals

MDPI

Article

Corrosion and Cavitation Performance of Flame-Sprayed NiCrBSi Composite Coatings Reinforced with Hard Particles

Doina Frunzaverde [1], Gabriela Marginean [2] and Costel Relu Ciubotariu [1,*]

[1] Department of Engineering Science, Faculty of Engineering, Babeș-Bolyai University, Square Traian Vuia 1-4, 320085 Resita, Romania; doina.frunzaverde@ubbcluj.ro
[2] Institute of Mechanical Engineering, Westphalian University of Applied Sciences Gelsenkirchen Bocholt Recklinghausen, Neidenburger Str. 43, 45897 Gelsenkirchen, Germany; gabriela.marginean@w-hs.de
* Correspondence: relu.ciubotariu@ubbcluj.ro

Abstract: To enhance the operational life of hydraulic machinery, protective coatings against wear, particularly cavitation erosion, and corrosion might be applied on the surfaces of components. The experiments conducted in this study aimed to assess the suitability of 80/20 NiCrBSi/WC-Co composite coatings for this purpose. A coating of NiCrBSi self-fluxing alloy, which served as the reference material, was deposited alongside a NiCrBSi coating reinforced with 20% WC-Co, both applied by flame spraying onto X3CrNiMo13-4 substrates, the martensitic stainless steel type frequently utilized in turbine blade manufacturing. The improved density of the coatings and adhesion to the substrate was achieved by remelting with an oxyacetylene flame. The cavitation and corrosion performance of both the reference and composite coating were evaluated through cavitation tests and electrochemical measurements conducted in the laboratory. The results demonstrate that the addition of 20% WC-Co significantly enhances the cavitation resistance of the composite material, as evidenced by the reduction to 3.76 times of the cumulative erosion (CE), while the stabilization rate remained at half the value observed for the reference self-fluxing alloy coating. Conversely, the addition of WC-Co into the NiCrBSi coating resulted in a slight decrease in the corrosion resistance of the self-fluxing alloy. Nevertheless, the corrosion rate of the composite coating (124.80 µm/year) did not significantly exceed the upper limit for excellent corrosion resistance (100 µm/year).

Keywords: cavitation resistance; corrosion resistance; coatings; hydraulic machinery; self-fluxing alloys; NiCrBSi; WC-12Co; NiCrBSi/WC-Co composites

check for updates

Citation: Frunzaverde, D.; Marginean, G.; Ciubotariu, C.R. Corrosion and Cavitation Performance of Flame-Sprayed NiCrBSi Composite Coatings Reinforced with Hard Particles. *Crystals* **2024**, *14*, 1078. https://doi.org/10.3390/cryst14121078

Academic Editor: Andrey Chumaevskii

Received: 7 November 2024
Revised: 4 December 2024
Accepted: 11 December 2024
Published: 13 December 2024

Copyright: © 2024 by the authors. Licensee MDPI, Basel, Switzerland. This article is an open access article distributed under the terms and conditions of the Creative Commons Attribution (CC BY) license (https://creativecommons.org/licenses/by/4.0/).

1. Introduction

Components of hydraulic machinery are exposed to extreme working conditions, characterized by high mechanical loads in environments that are commonly both corrosive and erosive. The material's quality, part design, manufacturing, and assembly processes therefore need special attention in order to avoid failure of the components during operation and thereby long-time downtime and high repair costs [1,2]. Despite ongoing design improvement, development of fabrication processes, the utilization of superior stainless steel materials, and the advancements in coatings designed for protection and deposition technologies, hydraulic turbine components continue to fail because of fatigue [3], corrosion, and wear, in particular cavitation erosion. Cavitation is a major cause of turbine damage, particularly in reaction turbines (like Kaplan turbines) [1].

The surface damage on the blades often leads to turbine vibrations, which can result in fatigue cracking of the runner blade [1]. Various methods have been developed to protect hydraulic machinery from the above-mentioned phenomenon, focusing on surface treatments (shot peening, plasma nitriding, deep rolling, and laser treatments [4]), deposition of coatings, and monitoring techniques. While the methods relying on surface engineering aim to enhance the superficial hardness of the component [4,5], monitoring methods

are crucial for early detection and suppression of cavitation, ensuring the machinery's operational safety and efficiency [6]. However, when considering the desired properties of a component's surface, previous research indicates that cavitation erosion resistance is influenced not only by hardness but also by further factors such as fatigue strength, ductility, and fracture toughness. Moreover, for coated components, this resistance is shown to depend on both the substrate's nature and the coating material's composition and structure [4].

Additionally, it has been noted that incorporating hard particles into a ductile matrix to enhance wear resistance may actually reduce cavitation erosion resistance [4]. To protect hydraulic components against cavitation and corrosion, several types of coatings are commonly used. These coatings help extend the lifespan of hydraulic components by providing a durable barrier against the two damaging environmental aggressions. The most frequently used coating materials are as follows:

- Carbide Coatings: These include tungsten carbide (WC), chromium carbides (Cr_3C_2, CrC), and mixtures of different carbides (20CrC-80WC). They are remarkable for their outstanding hardness and wear resistance [7], but their cavitation resistance is inferior to metallic materials like grey cast iron and hardly comparable to stainless steels, and moreover, the adhesion and thickness of the coatings are critical factors influencing their performance [8].
- Cermet Coatings: These are composite materials made of a ceramic phase including a metallic binder material. The ceramic components (e.g., carbides like WC, Cr_3C_2, TiC, ZrC, SiC, and Mo_2C) contribute to the coating hardness [9], while the metallic binders (typically Co, Co-Cr, Ni, Cr, and Ni-Cr) provide the required toughness [10–12]. HVOF-sprayed (High-Velocity Oxy-Fuel-sprayed) cermet coatings, such as WC-12Co, WC-10Co-4Cr, and Cr_3C_2-NiCr, exhibit excellent cavitation erosion resistance due to their high hardness, toughness, and low porosity. These coatings can also form protective oxides in corrosive environments, enhancing thereby their performance, as shown by previous research [13,14]. Particularly, although the WC-12Co coatings are reported to ensure good cavitation erosion resistance [15–18], one has to consider that the Co binder for the tungsten carbide does not provide the expected protection against corrosion [7,10,17,19,20]. In order to overcome this drawback, materials like Ni, Cr, or Ni-Cr can be added to the Co binder or can be used as complete replacements [10].
- Elastomeric Coatings: These coatings are designed to bond well to substrates and have elastomeric properties that help dissipate the energy from cavitation, reducing damage. Polymeric coatings are particularly useful because they can be applied to fully immersed surfaces and provide a flexible barrier that can absorb the impact of cavitation bubbles [21]. Enhanced cavitation resistance might be obtained by reinforcement of polymeric coatings like elastomers, epoxy resins, and polyurethane, with agents such as ceramics or metal particles. This combination improves the mechanical properties and durability of the coating.

Based on the results of all of these investigations, we can say that composite coatings reduce cavitation erosion by achieving superior mechanical and structural properties of the base materials. The addition of ceramic or metal particles contributes to increasing the microstructural density and reducing porosity, thus resulting in an increased resistance to cavitation wear.

Self-fluxing NiCrBSi coatings are effective at enhancing corrosion resistance, but they often fall short in wear resistance compared to ceramic materials. The phenomenon of adhesive wear in NiCrBSi coatings is responsible for considerable material loss despite the coatings exhibiting a relatively high hardness [22]. However, their relatively low melting temperature positions them as particularly suitable for use as a primary binder, enabling efficient wetting, adhesion, and binding of reinforcing particles. To improve wear resistance, studies have explored the addition of hard carbides, such as WC, to these coatings.

Specifically, investigations have been conducted on mixtures of NiCrBSi powders combined with different proportions of WC-12Co powders. These studies have demonstrated

that reinforcing NiCrBSi self-fluxing alloys with tungsten carbides enhances hardness and wear resistance [22–24]. Additionally, these reinforced coatings offer advantages over WC-CoCr or WC-Co layers in practice, requiring a more ductile coating [25]. Moreover, previous research reports about the fact that the addition of WC-Co in NiCrBSi alloys significantly influences the microstructure, mechanical properties, and resistance to the wear and corrosion of the resulting composites in direct correlation to the added WC-Co concentrations as follows:

- Low WC-Co Content (up to 15 wt%): Coatings with a low WC-Co content tend to have a more uniform and dense microstructure with fewer defects and lower porosity (around 0.6%). These coatings exhibit good hardness and moderate wear resistance. Their corrosion resistance is good due to the uniform distribution of phases and lower porosity [26].
- Medium WC-Co Content (15 wt% to 30 wt%): Increasing the WC-Co content to this range enhances the hardness and wear resistance of the coatings. Coatings in this range show a balance between hardness and toughness, leading to improved overall performance. The corrosion resistance remains good, but the increased hardness can sometimes lead to micro-cracks, which may slightly reduce corrosion resistance [26].
- High WC-Co Content (30 wt% to 60 wt%): A high WC-Co content results in a more complex microstructure. These coatings have the highest hardness and wear resistance but might become more brittle. On the other hand, while the wear resistance is significantly improved, the corrosion resistance can be compromised due to the increased brittleness and potential for micro-cracks [27].

In summary, the optimal WC-Co content depends on the specific application requirements. For applications requiring high wear resistance and hardness, a higher WC-Co content (around 30 wt% to 60 wt%) is beneficial, while for applications where toughness and lower brittleness are crucial, a medium WC-Co content (15 wt% to 30 wt%) might be more suitable. On the other hand, one has to consider that a higher WC-Co content may slightly reduce corrosion resistance in very aggressive environments (such as those containing chlorides). WC particles may undergo some form of degradation or galvanic corrosion at the interface between WC and the NiCrBSi matrix. This effect can slightly reduce corrosion resistance if the WC content is too high.

Given the above, it can be assumed that NiCrBSi/WC-Co composites with a medium WC-Co content, subsequently remelted after flame spraying, to improve the coating quality and adhesion to the metallic substrate, could be an effective solution for protecting hydraulic components against cavitation and corrosion. This topic has been previously addressed in only two studies. In [28], the authors compared two WC-NiCrBSi coatings, obtained by vacuum cladding of different raw materials, in terms of their microstructure and resistance to corrosion and cavitation. In [29], two compositions of NiCrBSi/WC-Co, respectively, 85/15 and 70/30, fabricated by flame spraying and remelting, were compared regarding their microstructure and the behavior of cavitation and corrosion. The properties of the coating with a 15% addition of WC-Co were shown to be superior to those of the coating with a higher content of WC-Co (30%).

Balancing the ratio between the two components (NiCrBSi and WC-Co) helps improve the coatings' overall performance in conditions where both wear resistance and corrosion resistance are essential. Materials like tungsten carbide can be added up to a certain amount to a metallic matrix because they are more susceptible to cracking, especially under high stress (they are extremely hard but have low fracture toughness).

Considering the above mentioned, one may conclude that there is extensive research regarding the phase constitution, microstructure, and sliding wear resistance of NiCrBSi/WC-Co composite coatings, but only very few studies are addressing the cavitation resistance and, even less so, both the cavitation resistance and the corrosion resistance of self-fluxing alloys reinforced with hard particles. Regarding the deposition methods of the protective coatings, previous research focused on laser cladding, vacuum cladding, APS, supersonic plasma spraying, HVOF, and HVOAF.

Aiming to determine if flame-sprayed and successive flame-remelted NiCrBSi/WC-Co coatings can provide simultaneous protection of Kaplan turbine runner blades against cavitation and corrosion, the authors of the present study evaluated the microstructure, the hardness, the cavitation resistance, and the corrosion behavior of the composite coating with 20% WC-Co in comparison with those of the self-fluxing coating (NiCrBSi), considered to be the reference material.

2. Materials and Methods

A NiCrBSi/WC-Co composite coating, consisting of a NiCrBSi self-fluxing alloy (SFA/M-772.91 powder, −106 + 45 µm from the Company FST, Duiven, The Netherlands) with 20% addition of a hard metal powder (WC-Co, −45 + 15 µm from GTV Company, Luckenbach, Germany) was applied by flame spraying on a martensitic stainless steel substrate (type X3CrNiMo13-4). The powder mixture used for deposition was achieved by means of a mechanical mixing technique. To highlight the influence of WC-Co reinforcement, a reference layer made of 100% SFA was also deposited. The sample denominations used in this research and the corresponding feedstock powder compositions can be visualized in Table 1.

Table 1. Feedstock powder composition for the coating deposition.

Sample	Coating Powder (in wt. %)
80/20	80% Ni–Cr–B–Si + 20% WC-Co
SFA	100% Ni–Cr–B–Si

Before spraying, the surface of the stainless steel substrate (X3CrNiMo13-4) was roughened using a sand-blasting machine. To refine the layer morphology and enhance the adhesion of the coating to the substrate, a remelting treatment with an oxyacetylene flame at 1000 ± 10 °C was applied after thermal spraying. The flame spray process parameters were spray distance of 200 mm, oxygen flow of 1.6 m^3/h, and acetylene flow of 0.85 m^3/h.

Microstructural investigations of the coatings were conducted on cross-sectional samples by means of scanning electron microscopy (SEM/FEI Company, Philips XL 30 ESEM, Frankfurt am Main, Germany) combined with energy dispersive X-ray analysis (EDX from EDAX) and correlated with X-ray diffraction (XRD/Philips X'Pert Diffractometer, Panalytical, The Netherlands).

Hardness indentation measurements have been performed on cross-sectional samples using an Emco tester model M1C 010 (EMCO-TEST Prufmaschinen GmbH, Kuchl, Austria). To determine the Vickers hardness (8 indents), a load of 0.3 kgf was applied for 15 s.

To assess the corrosion resistance of the composite coating relative to the reference material, electrochemical measurements were carried out on disk-shaped samples with a diameter of 13 mm. Polarization curves were recorded in the positive direction at room temperature in a 3.5% NaCl solution, with three measurements registered for each material. A three-electrode cell was employed, featuring a saturated calomel electrode (SCE) as the reference and platinum serving as the counter electrode. The applied potential ranged from −1500 to 1000 mV (versus SCE) at a rate of 10 mV/min.

In this study, the cavitation tests were conducted using the vibratory indirect method in accordance with ASTM G-32. The specimen was securely fixed and completely submerged in the liquid.

The resonance frequency of the oscillator was maintained at 20 ± 0.5 kHz, while the double (peak-to-peak) amplitude of the vibrating sonotrode was set at 50 µm. De-ionized water served as the test liquid, which was maintained at room temperature using a control device and a cooling water system. Each new test specimen required the fluid vessel to be cleaned and filled with fresh liquid. The distance between the test specimen and the vibrating sonotrode was adjusted in accordance with prior research recommendations. The tested samples were periodically removed after predetermined time intervals, cleaned with

acetone, dried in airflow, and weighed with a precision balance (five decimal places). The test results were expressed as cumulative erosion (CE) values.

3. Results

3.1. Microstructural Characterization

The coatings' microstructure is presented in Figure 1, and the corresponding EDX analysis of the representative constituents observed can be visualized in Figure 2. The phase composition of the presented microstructure is displayed in Figure 3 and associated with the features marked in Figure 1d. There is a significant alignment between the identified phases and the findings presented by the EDX analysis.

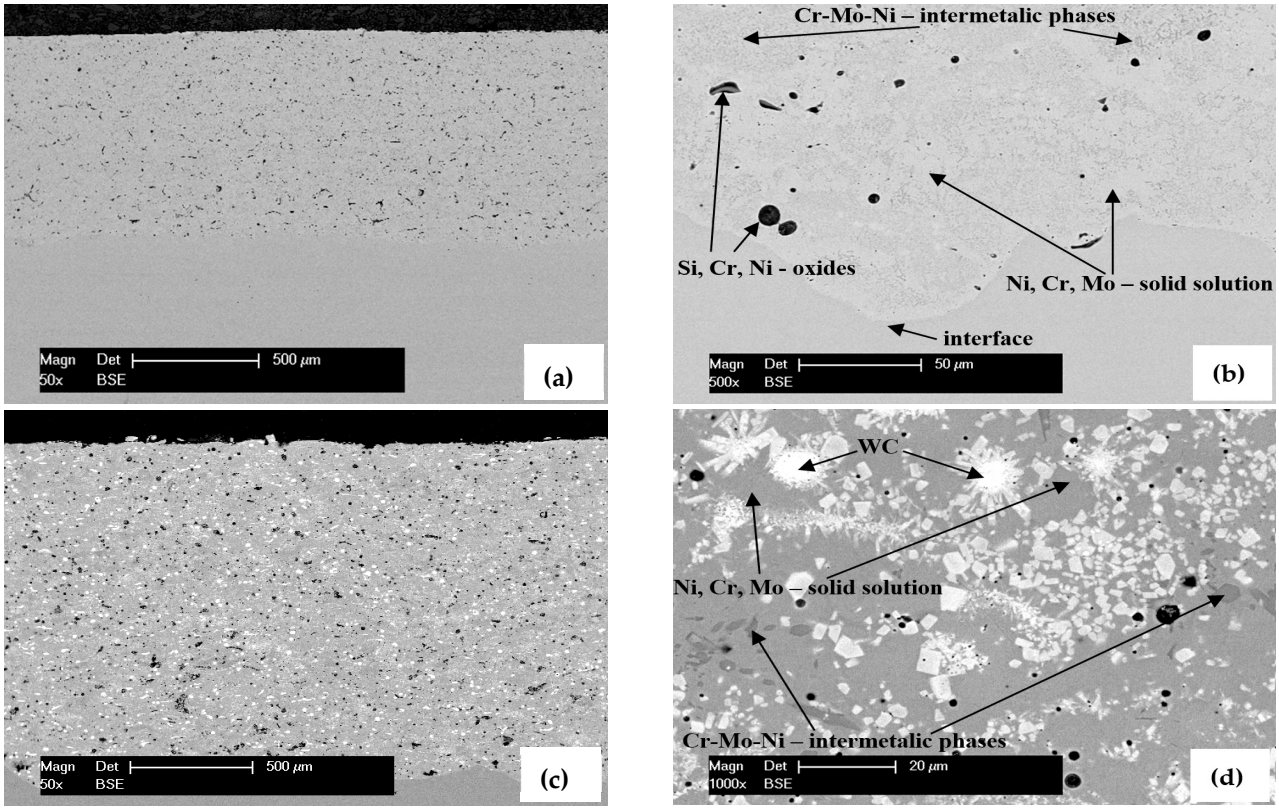


Figure 1. Cross-section SEM micrographs of the flame-sprayed and -remelted coating: SFA (**a**,**b**) and 80/20 (**c**,**d**).

The post-processed coatings are free of cracks and show a compact multi-phase microstructure with a homogenous phase distribution and good adhesion to the substrate. As revealed by the EDX 1 spectrum, the black globular formations are either gas agglomerations or residual slag microparticles, formed following the flame-remelting process, recording in their composition different types of oxides, such as Si, Cr, and/or Ni. The light gray constituent (EDX 2) has a finely dispersed structure and is composed of Ni, Cr, and Mo solid solutions with silicides and carbides. The dark gray formations (EDX 3) indicate some phases rich in Cr, Mo, and Ni.

The particles very light grey to white (EDX 4) represent tungsten carbide (WC). Elements like Cr and Ni belonging to the metallic matrix were also detected.

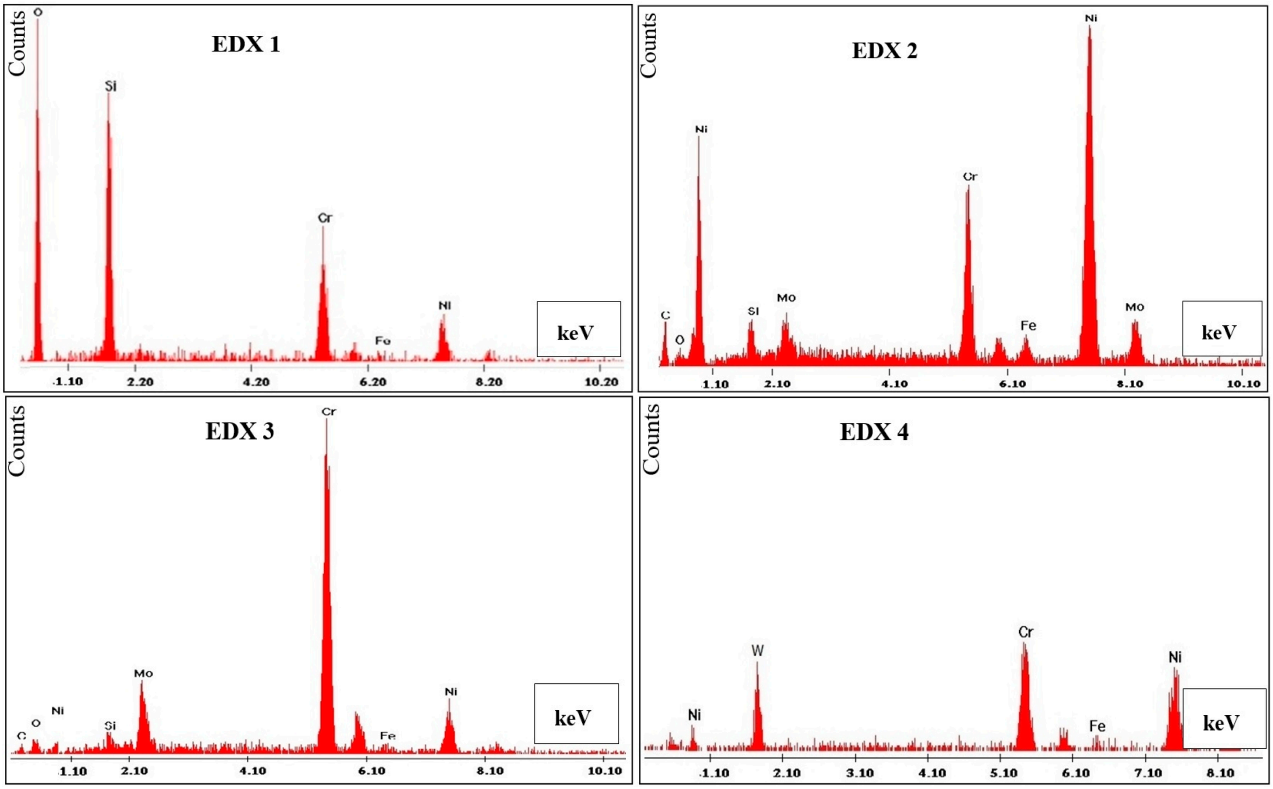


Figure 2. EDX analysis of the microstructural constituents marked in Figure 1b,d.

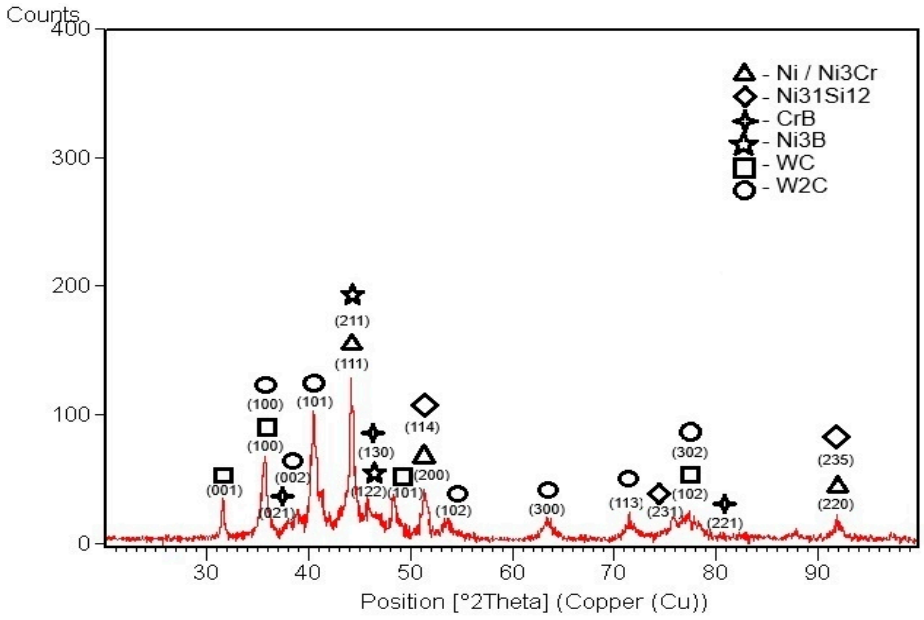


Figure 3. XRD pattern of the composite coating 80/20.

3.2. Hardness Tests

Table 2 shows the results of the hardness tests and the corresponding average values. While for the SFA layer, the resulting average value of the hardness was 622 (HV 0.3), the composite layer (80/20) exhibited a slightly lower average value associated with a higher standard deviation. This observation is explained by the higher susceptibility to crack formation in the region of the indents, respectively, on the local microstructural composition with different amounts of ceramic component.

Table 2. The micro-hardness values of the investigated layers [HV0.3].

Measurements	SFA	80/20
1.	593	540
2.	642	574
3.	585	592
4.	651	530
5.	659	635
6.	618	555
7.	604	517
8.	625	601
Average value and standard deviation	622 ± 27	568 ± 40

The hardness of the WC particles significantly exceeds that of the NiCrBSi matrix, which creates a mismatch in hardness that can result in stress concentration at the interface between the WC and the NiCrBSi matrix during indentation. Such stress concentration can facilitate the initiation of micro-cracks at the interfaces, particularly when the bonding between the WC and the matrix is suboptimal.

The occurrence of cracking during the indentation process may lead to a decrease in the apparent hardness values derived from an indentation test. When cracks develop, they can enlarge the size of the indentation region or affect the material's reaction to the indent. The presence of cracks at the periphery of the indentation may lead to an apparent increase in the diagonal measurement of the indentation, particularly in the context of Vickers hardness testing. The correlation between hardness and susceptibility to cracking is not linear. It is rather influenced by the trade-offs between hardness, toughness, and brittleness.

The microstructure of a material is essential in determining the correlation between the hardness and crack susceptibility. When materials possess finer grains or smaller particles of hard phases, such as tungsten carbide (WC), they typically demonstrate reduced crack susceptibility. This reduction is due to the more even distribution of stress concentrations across a larger surface area, which diminishes the probability of crack formation at any particular site.

Larger WC particles or their agglomerations (see Figure 1) are more prone to initiating cracks, as they function as sites of concentrated stress. Consequently, cracks are more likely to develop and extend along the boundaries between the particles and the matrix, thereby enhancing the overall brittleness of the material.

Therefore, the WC particle size, its distribution, and the balance to the metallic matrix are essential factors in enhancing toughness to mitigate the brittleness associated with the addition of tungsten carbide.

3.3. Corrosion Behavior

Using Tafel extrapolation of the polarization curves shown in Figure 4, the corrosion current density (icorr), the corrosion potential (Ecorr), and corrosion rate (Rcorr) were determined, as depicted in Table 3.

Table 3. Comparative presentation of the values obtained from the corrosion test.

Sample	E_{corr} [mV]	i_{corr} [μA/cm^2]	R_{corr} [μm/year]
SFA	−27.00	4.49	52.53
80/20	−211.50	12.22	124.80

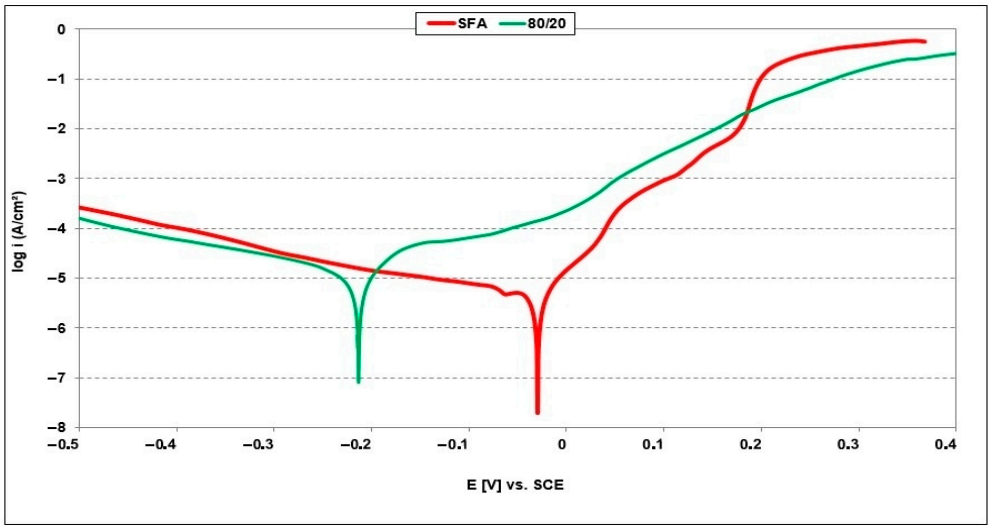


Figure 4. Current density vs. potential curves of the coatings (SFA compared to 80/20) evaluated in a 3.5% NaCl solution.

The Ecorr values can be directly linked to the coating's chemical composition, particularly the elements like Co, Ni, or Cr, responsible for the variation in the corrosion behavior. NiCrBSi exhibits excellent corrosion resistance attributed to the development of stable passive layers, such as chromium oxide, which protect the material against further corrosion attacks in various environments.

As one may observe, the inclusion of the hard phases in the NiCrBSi layer noticeably shifted the Ecorr values towards the cathodic domain (left). This phenomenon was to be expected, as the presence of WC particles generates new interfaces with the metallic matrix that might result in a slight reduction in corrosion resistance when exposed to very aggressive environments, such as those containing chlorides. Furthermore, the WC particles may initiate degradation or galvanic corrosion at the junction with the NiCrBSi matrix, potentially leading to a further decrease in the corrosion resistance if the WC content exceeds a critical limit, as shown in [28].

The results obtained for the icorr values show an increase of approximately three times for the composite coating 80/20 in comparison with the values recorded for the SFA coating. Furthermore, it can be observed that with the addition of 20% hard phases in the layer, the value of the corrosion rate increased to 124,80 μm/year but still maintained in the range considered to denote good corrosion behavior for industrial application in a chloride environment (around 100 μm/year). This observation is valid just in the case of a homogeneous corrosion attack. For localized corrosion attacks, the penetration depth must be taken into consideration, as well.

Therefore, in order to evaluate the overall effect of the reinforcement with hard particles on the corrosion resistance of the NiCrBSi matrix, the microstructures of the cross-sections of the corroded coatings were also compared with each other (Figure 5).

As revealed by Figure 5, the penetration depth of the corrosion attack increased from 15.6 μm for the SFA coating up to 121 μm for the 80/20 composite coating. These phenomena can be explained based on the potential differences between the two structural components with different chemical compositions (the self-fluxing material in contact with the ceramic component). At any interface between the ceramic phase and the intermetallic phase, a galvanic microcell is formed in the presence of a corrosive environment, where the intermetallic phase becomes the anode and the ceramic phase acts as the cathode.

Moreover, in Figure 5 we can also visualize the presence of local corrosive attack, respectively the appearance of the pitting phenomenon. This is a consequence of the fact that the cobalt binder in WC-Co exhibits a vulnerability to pitting and crevice corrosion in chloride solutions, which diminishes the composite's overall corrosion resistance. The

corrosion of cobalt results in the exposure of WC particles, potentially compromising structural integrity and accelerating material degradation. By lowering the WC-Co content, the exposure of cobalt to chloride attack can be minimized, which allows the more corrosion-resistant NiCrBSi matrix to dominate on the surface. This alteration results in improved corrosion resistance in chloride solutions, but it will compromise wear resistance. Therefore, balancing the ratio between these two components is crucial for obtaining composite coatings with improved wear behavior and without significant negative influence on good corrosion resistance.

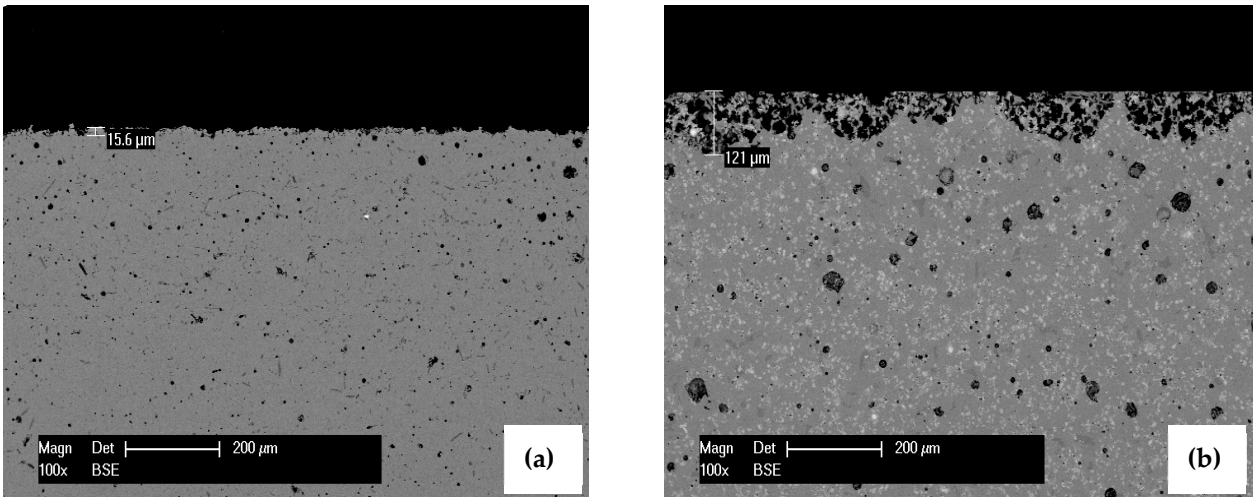


Figure 5. Cross-sectional SEM micrographs of the coatings following electrochemical corrosion testing, highlighting the penetration depth of the corrosion attack: (**a**) SFA and (**b**) 80/20.

3.4. Cavitation Erosion Behavior

The cavitation erosion behavior of the two types of coatings (SFA and 80/20) was evaluated by means of the vibration method standardized by ASTM G-32 [30]. For reproducibility, the tests were conducted on several samples over a duration of 1800 min under identical conditions. The testing period has been divided into 67 intervals for the weighing process. Figure 6 shows the average value of the total eroded mass [Δm] for three samples of each coating type as a function of the duration of exposure to cavitation.

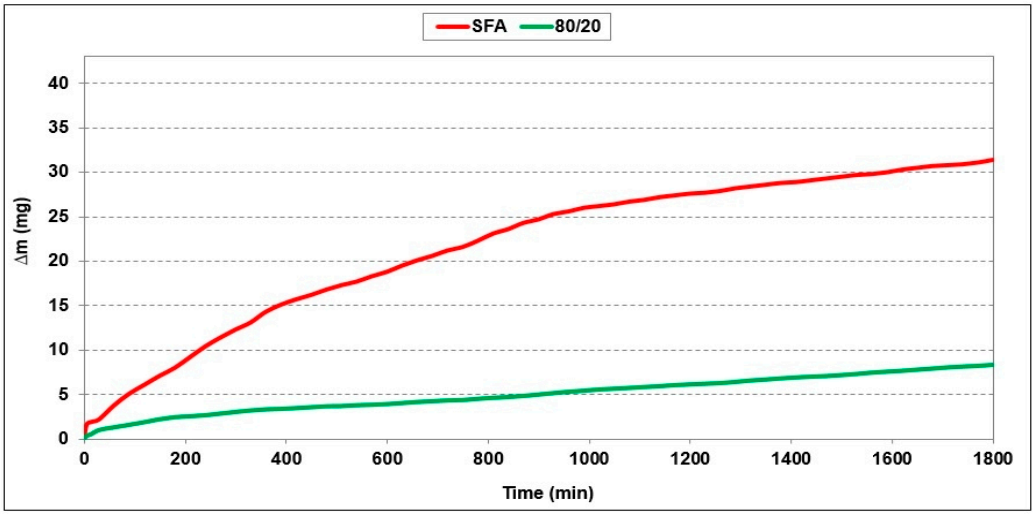


Figure 6. Variation of eroded mass for the samples exposed to cavitation erosion up to 1800 min.

Cumulative erosion values (CE) and stabilization rate values (Vs) were determined for all cavitation erosion-tested coatings. The parameter that can be considered independent of

the roughness of the eroded surface and the initial material losses in the accumulation zone is Vs. From this point of view, it is recommended to compare the layers according to the erosion rate in the stabilization zone [31]. Table 4 shows the calculated values for CE and vs. according to ASTM G-32.

Table 4. Cumulative erosion (CE) and terminal erosion rate (Vs) after 1800 min of cavitation exposure.

Measurements	SFA	80/20
CE [mg]	31.40	8.36
Vs $\times 10^{-3}$ [mg/min]	7.44	3.89

The results from Figure 6 and Table 4 clearly show that reinforcing NiCrBSi with 20% WC-Co significantly enhanced the cavitation resistance of the composite coating. After 1800 min of cavitation exposure, the cumulative erosion (CE) of the 80/20 composite coating was 3.76 times lower than that of the NiCrBSi coating. Additionally, the stabilization rate (Vs) was maintained at 3.89 $\times$ 10^{-3} mg/min, which is less than half the reference value of the self-fluxing coating, 7.44 $\times$ 10^{-3} mg/min. These values are in accordance with the results obtained by the authors of [29], demonstrating the superiority in terms of cavitation resistance of the 80/20 coating in comparison to both the 85/15 and the 70/30 NiCrBSi/WC-Co composite coatings.

4. Conclusions

The experiments conducted by the authors of this paper indicate that 80% NiCrBSi/20% WC-Co flame-sprayed and -remelted composite coatings are effective for protecting hydraulic machinery against cavitation and can also provide acceptable corrosion resistance. Previous research [1] has shown that cavitation is one of the main external causes of reaction-type turbine damage, often followed by corrosion and fatigue cracking. Therefore, NiCrBSi coatings reinforced with 20% WC-Co might be considered an acceptable solution for surface protection of Kaplan turbine blades.

Thus, reinforcing NiCrBSi with 20% WC-Co significantly increased the cavitation erosion resistance of the resulting 80/20 composite coating. The cumulative erosion (CE) was reduced by 3.76 times, and the stabilization rate was maintained at half the value observed for the reference SFA coating.

Although the addition of 20% WC-Co increased the corrosion rate, the value for the investigated composite coating is not significantly higher than the generally accepted upper limit for similar applications in salt water (100 µm/year).

The results obtained from the experimental determinations are in complete accordance with the findings of [29] and complete the information with the results regarding the cavitation erosion of NiCrBSi alloys reinforced with medium WC-Co content (15 wt% to 30 wt%).

Author Contributions: Conceptualization, C.R.C.; methodology, G.M. and D.F.; formal analysis, G.M. and D.F.; investigation, C.R.C. and G.M.; resources, C.R.C., G.M. and D.F.; writing—original draft preparation, C.R.C. and D.F.; writing—review and editing, C.R.C., D.F. and G.M.; visualization, D.F. and G.M.; funding acquisition, C.R.C. and G.M. All authors have read and agreed to the published version of the manuscript.

Funding: This research received no funding.

Data Availability Statement: The data presented in this study are available on request from the corresponding author.

Acknowledgments: The authors wish to express their gratitude to the company Karl Schumacher GmbH, Essen, Germany, for the deposition of the coatings.

Conflicts of Interest: The authors declare no conflict of interest.

References

1. Khalid Mohammed Ridha, W.; Reza Kashyzadeh, K.; Ghorbani, S. Common Failures in Hydraulic Kaplan Turbine Blades and Practical Solutions. *Materials* **2023**, *16*, 3303. [CrossRef]
2. Câmpian, V.C.; Frunzaverde, D.; Nedelcu, D.; Marginean, G. Failure Analysis of a Kaplan Turbine Runner Blade. In Proceedings of the 24th IAHR Symposium on Hydraulic Machinery and Systems, Foz do Iguassu, Brazil, 27–31 October 2008.
3. Ciubotariu, C.R.; Secosan, E.; Marginean, G.; Frunzaverde, D.; Campian, V.C. Experimental Study Regarding the Cavitation and Corrosion Resistance of Stellite 6 and Self-Fluxing Remelted Coatings. *Stroj. Vestn. J. Mech. Eng.* **2016**, *62*, 154–162. [CrossRef]
4. Krella, A.K. Degradation and Protection of Materials from Cavitation Erosion: A Review. *Materials* **2023**, *16*, 2058. [CrossRef]
5. Selvam, K.; Mandal, P.; Grewal, H.; Arora, H. Ultrasonic cavitation erosion-corrosion behavior of friction stir processed stainless steel. *Ultrason. Sonochem.* **2018**, *44*, 331–339. [CrossRef] [PubMed]
6. Zhu, Y.; Zhou, L.; Lv, S.; Shi, W.; Ni, H.; Li, X.; Tao, C.; Hou, Z. Research Progress on Identification and Suppression Methods for Monitoring the Cavitation State of Centrifugal Pumps. *Water* **2023**, *16*, 52. [CrossRef]
7. Singh, R.; Tiwari, S.K.; Mishra, S.K. Cavitation Erosion in Hydraulic Turbine Components and Mitigation by Coatings: Current Status and Future Needs. *J. Mater. Eng. Perform.* **2012**, *21*, 1539–1551. [CrossRef]
8. Qiu, N.; Wang, L.; Wu, S.; Likhachev, D. Research on cavitation erosion and wear resistance performance of coatings. *Eng. Fail. Anal.* **2015**, *55*, 208–223. [CrossRef]
9. Pogrebnyak, A.D.; Tyurin, Y.N. Modification of material properties and coating deposition using plasma jets. *Phys. Usp.* **2005**, *48*, 487–514. [CrossRef]
10. Govande, A.R.; Chandak, A.; Sunil, B.R.; Dumpala, R. Carbide-based thermal spray coatings: A review on performance characteristics and post-treatment. *Int. J. Refract. Met. Hard Mater.* **2021**, *103*, 105772. [CrossRef]
11. Mishra, T.K.; Kumar, A.; Sinha, S.K. Experimental investigation and study of HVOF sprayed WC-12Co, WC-10Co-4Cr and Cr3C2-25NiCr coating on its sliding wear behavior. *Int. J. Refract. Met. Hard Mater.* **2021**, *94*, 105404. [CrossRef]
12. Kumar, K.; Kumar, S.; Singh, G.; Singh, J.P.; Singh, J. Erosion Wear Investigation of HVOF Sprayed WC-10Co4Cr Coating on Slurry Pipeline Materials. *Coatings* **2017**, *7*, 54. [CrossRef]
13. Liu, J.; Chen, T.; Yuan, C.; Bai, X. Performance Analysis of Cavitation Erosion Resistance and Corrosion Behavior of HVOF-Sprayed WC-10Co-4Cr, WC-12Co, and Cr3C2-NiCr Coatings. *J. Therm. Spray Technol.* **2020**, *29*, 798–810. [CrossRef]
14. Mayer, A.; Bertuol, K.; Siqueira, I.; Chicoski, A.; Váz, R.; Sousa, M.; Pukasiewicz, A. Evaluation of cavitation/corrosion synergy of the Cr3C2-25NiCr coating deposited by HVOF process. *Ultrason. Sonochem.* **2020**, *69*, 105271. [CrossRef] [PubMed]
15. Liu, J.; Bai, X.; Chen, T.; Yuan, C. Effects of Cobalt Content on the Microstructure, Mechanical Properties and Cavitation Erosion Resistance of HVOF Sprayed Coatings. *Coatings* **2019**, *9*, 534. [CrossRef]
16. Du, J.; Zhang, J.; Zhang, C. Effect of Heat Treatment on the Cavitation Erosion Performance of WC–12Co Coatings. *Coatings* **2019**, *9*, 690. [CrossRef]
17. Ding, X.; Ke, D.; Yuan, C.; Ding, Z.; Cheng, X. Microstructure and Cavitation Erosion Resistance of HVOF Deposited WC-Co Coatings with Different Sized WC. *Coatings* **2018**, *8*, 307. [CrossRef]
18. Lamana, M.S.; Pukasiewicz, A.G.M.; Sampath, S. Influence of cobalt content and HVOF deposition process on the cavitation erosion resistance of WC-Co coatings. *Wear.* **2018**, *398-399*, 209–219. [CrossRef]
19. Torkashvand, K.; Joshi, S.; Gupta, M. Advances in Thermally Sprayed WC-Based Wear-Resistant Coatings: Co-free Binders, Processing Routes and Tribological Behavior. *J. Therm. Spray Technol.* **2022**, *31*, 342–377. [CrossRef]
20. Luiz, L.A.; de Andrade, J.; Pesqueira, C.M.; de Araujo, I.B.; Siqueira, F.; Sucharsk, G.B.; de Sousa, M.J. Corrosion Behavior and Galvanic Corrosion Resistance of WC and Cr3C2 Cermet Coatings in Madeira River Water. *J. Therm. Spray Technol.* **2021**, *30*, 205–221. [CrossRef] [PubMed]
21. Ciubotariu, C.-R.; Frunzaverde, D. Cavitation Resistance of Elastomeric Coatings Deposited by Different Methods. *Mater. Plast.* **2019**, *56*, 875–881. [CrossRef]
22. Bergant, Z.; Batič, B.Š.; Felde, I.; Šturm, R.; Sedlaček, M. Tribological Properties of Solid Solution Strengthened Laser Cladded NiCrBSi/WC-12Co Metal Matrix Composite Coatings. *Materials* **2022**, *15*, 342. [CrossRef] [PubMed]
23. Rachidi, R.; Kihel, B.E.; Delaunois, F. Microstructure and mechanical characterization of NiCrBSi alloy and NiCrBSi-WC composite coatings produced by flame spraying. *Mater. Sci. Eng. B* **2019**, *241*, 13–21. [CrossRef]
24. Vencl, A.; Mrdak, M.; Hvizdos, P. Tribological properties of WC-Co/NiCrBSi and Mo/NiCrBSi plasma spray coatings under boundary lubrication conditions. *Tribol. Ind.* **2017**, *39*, 183–191. [CrossRef]
25. Pulsford, J.; Venturi, F.; Kamnis, S.; Hussain, T. Sliding wear behaviour of WC-Co reinforced NiCrFeSiB HVOAF thermal spray coatings against WC-Co and Al_2O_3 counterbodies. *Surf. Coat. Technol.* **2020**, *386*, 125468. [CrossRef]
26. Guo, H.; Li, B.; Lu, C.; Zhou, Q.; Jia, J. Effect of WC–Co content on the microstructure and properties of NiCrBSi composite coatings fabricated by supersonic plasma spraying. *J. Alloys Compd.* **2019**, *789*, 966–975. [CrossRef]
27. Tabatabaei, F.S.K.; Ghasemi, B.; Mirzaee, O.; Adabifiroozjaei, E. The effect of WC-CoCr content on hardness and tribological properties of NiCrBSi coatings fabricated by the HVOF process. *Surf. Coat. Technol.* **2023**, *466*, 129506. [CrossRef]
28. Zhang, H.F.; Zhang, C.H.; Wang, Z.Y.; Cui, X.; Zhang, S.; Chen, H.T. Microstructure and corrosion behaviour of WC/NiCrBSi coatings by vacuum cladding. *Mater. Sci. Technol.* **2022**, *38*, 19–29. [CrossRef]
29. Ciubotariu, C.; Frunzaverde, D.; Mărginean, G. Investigations of Cavitation Erosion and Corrosion Behavior of Flame-Sprayed NiCrBSi/WC-12Co Composite Coatings. *Materials* **2022**, *15*, 2943. [CrossRef] [PubMed]

30. *ASTM G32*; Standard Test Method for Cavitation Erosion Using Vibratory Apparatus. ASTM International: West Conshohocken, PA, USA, 2010.
31. Secosan, E.R.; Ciubotariu, R.C.; Cojocaru, V.; Frunzaverde, D.; Câmpian, C.V. Study Regarding the Cavitation Erosion Behaviour and Residual Stresses of Impact Resistant Hardfacing Materials. *Adv. Mater. Res.* **2014**, *1029*, 146–151. [CrossRef]

Disclaimer/Publisher's Note: The statements, opinions and data contained in all publications are solely those of the individual author(s) and contributor(s) and not of MDPI and/or the editor(s). MDPI and/or the editor(s) disclaim responsibility for any injury to people or property resulting from any ideas, methods, instructions or products referred to in the content.